

# Conception of Magnetic Memory Switched by Time Dependent Current Density and Current Electron Spin Polarization

P. Steblinski, T. Blachowicz

**Abstract**—In this article the magnetic memory model with nano-meter size made from iron cells was proposed. For a purpose of determining the model specifications, the magnetic probes group with different geometrical parameters were examined using numeric simulations for the two different time duration of transitions among quasi-stable magnetic distributions found in the system, derived from the energy minimums. The geometrical parameters range was found, for which the 16 quasi-stable energetic states exist for the each probe. Having considered these results the 4 bits magnetic cells systems can be designed whose state is changed by spin-polarized current. Time dependent current densities and the current electron spin polarization directions were determined for all cases of transitions among quasi-stable states, for discovered set of 4 bits cells with different geometrical parameters. The 16-states cells, with the least geometrical area, achieved the 300 times bigger writing density in comparison to actual semiconductor solutions with the largest writing densities. The transitions among quasi-stable states of cells were examined for the time durations  $10^5$  times shorter than that for up to date solutions.

**Keywords**—spintronics, magnetic logic, BPM memories, magnetic simulations

## I. INTRODUCTION

**I**MPORTANT topic considered in spintronics is construction of signal processing devices, generators, and magnetic memories which may have better performance and speed in comparison to actual semiconductor devices or devices based on thick continuous magnetic layers. Some research teams still focus on MRAM memories formulation, the topic begun in early 90's [1]. The other teams carry research in areas of racetrack memories, which are based on domain wall evolution in semiconductor embedded nanowires [2]. The similar idea, to the racetrack one, was to allocate more than one bit in a single magnetic cell [3]. Actually, there exist research capabilities to obtain the magnetic memories construction based on BPM (bit-patterned media) [4]. Combining the BPM memory idea with memory cell idea where one can put many bits in a single cell, seems very

challenging, while some research teams obtained adequate results with nanomagnetic cells compatible with actual solutions for reading/writing heads [5 – 8]. Having continued the similar research direction, one has focused on the examination of the magnetic cells set which has had adaptive geometrical parameters in order to obtain multi-state, thus multi-bit memory cell with as small as possible size. The adaptation of cell sizes address the very recent topic of neuro-inspired computations, where the computing unit can be active like a neuron. Also, the geometrical size decrease gives the expectancy to obtain the larger writing density and shorter quasi-stable transition-time than that used in actual memory constructions. The visual memory model based on magnetic cells set, with many quasi-stable energetic states, is shown on Fig.1.

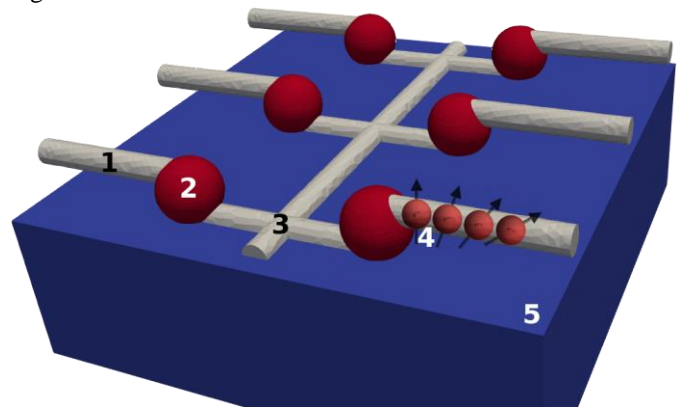


Fig. 1. Visualization of the magnetic cell system model with many quasi-stable states found in energetic minimum of the device. The state is changed by the time variable spin-polarized current density. Descriptions: conductive nonmagnetic junction (1), conductive multistate magnetic cell (2), conductive nonmagnetic junction (3), a change of the system state is induced by the spin-electron current with the time adjustable density and the spin polarization (4), nonmagnetic substrate (5).

The system state-change is performed using current which flows via cell and which has time-dependent flow density of spin-polarized electrons. After the recognition of the existing quasi-stable magnetisation distributions (treated as the memory states) in the system, distinguished by the calculated energy minimums, one should determine the system exciting signals in order to enforce transitions between quasi-stable states of the given cell. As it is well known, in order to keep control over the magnetic systems, using such external signal, a proper time and space dependent external magnetic field should be applied. As it was shown in [8–9], the magnetization evolution and thus the necessary for its adaptation (excitation), by externally applied magnetic field,

The work was partially supported by the SUT Rector Grant 14/990/RGJ18/0099 and the internal SUT project BK-229/RIF/2017.

P. Steblinski is with Department of Electronic and Informatics, Koszalin University of Technology (e-mail: psteb@bobolin.com.pl).

T. Blachowicz is with Institute of Physics – CSE, Silesian University of Technology (e-mail: tomasz.blachowicz@polsl.pl).

depends on (among others) the magnetic object geometrical shape and the object construction material. One should expect that when magnetic system is controlled by spin-polarized current – its density and the electrons spin polarization direction depends on many factors like: cell shape, construction material and a time of transition between quasi-stable cell states. So the adjustment of these parameters to obtain many quasi-stable energetic states and the proper transitions among these states, under the influence of spatially homogeneous current density and polarization, can be the serious research challenge.

## II. SIMULATIONS

In order to obtain desired results, usually the cycle of  $10^3$  micromagnetic simulations for the group of probes, was performed. The algorithm of computation was schematically shown in Fig. 2. It was discovered, that for the 16 quasi-stable energetic states (with different magnetization distribution) the equivalent adaptable parameters from Fig. 2f (1054 simulations) indeed exist. Thus, the radius  $R$  was changed from 0.5 to 2.0 nm with the step of 0.05 nm. The cutting angle  $\alpha$ , describing the cell base dimension, was varied from 0 to 135 degrees with the step equal to  $0.05\pi$  radians. Next, the two cycles of 364 simulations, searching for geometrical optimum parameters, for which the 16 quasi-stable energetic states exist, for the two different times of transitions among these states (1 ps and 5 ps), were performed.

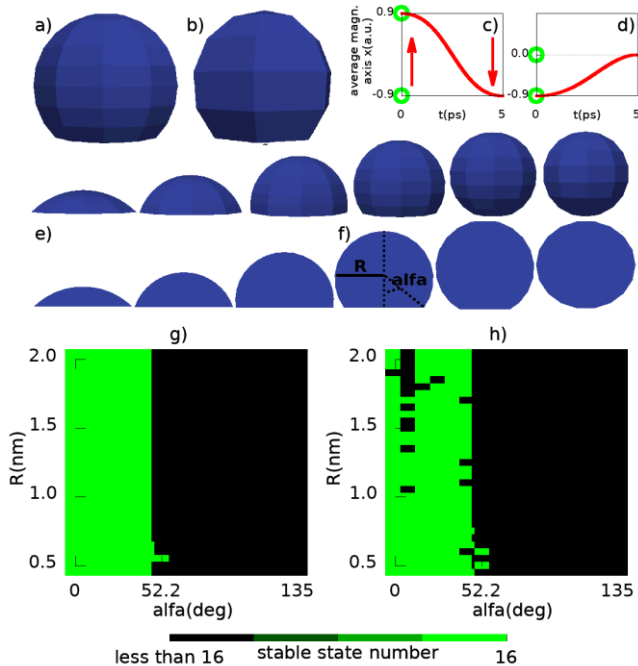


Fig. 2. The spherical shape (a), and the magnetic dot picture (b) approximated with 100, and 36 vertexes, respectively. Graphs of average (c), transient (d) magnetization for transition between quasi-stable states (green circle marked) for transition time 5ps for 100 vertexes object with radius 0.95 nm and alpha 0 degree. Approximated with 100 vertexes spherical object picture at the change of angle parameter alpha in section 0 -135 degree for some (e), selected angles from simulated angle domain, and under respectively - object sections marked on (f). The changeable parameters:  $R$  – object radius and  $\alpha$  – the cutting angle. Maps of examined geometrical parameters with green marked area for which it exists 16 quasi-stable energetic states for 100 vertexes (g) and 36 vertexes objects respectively (h).

Each of the 364 simulations consisted of the different excitation and the adequate transitions among the 16 quasi-stable energetic states, forwards and backwards, leading to 240 transitions scenarios. The simulations aimed determination the exciting current parameters (density and the spin polarization direction expressed in spherical coordinates). It was also determined the maximum percentage deviation between energies: the target energetic minimum and the energy obtained in the system after a simulation. The examined magnetic probes space was divided into finite elements according to Galerkin method. The simulations were performed using the modified MagPar [10] software, which was solving LLG equation including Slonczewski term in each step of simulation. Eq. 1 determines the evolution of magnetization, its space-time distribution, in a presence of the effective field (vector  $H_{eff}$ ), as well as in a presence of the Slonczewski term which includes density current  $j$  of electrons with spin polarized along the direction of vector  $p$  (Eq. 2) [11, 12].

$$\frac{1}{\gamma} \frac{d\vec{m}}{dt} = -\frac{1}{1+\alpha^2} [\vec{m} \times (\vec{H}_{eff} + \frac{jg}{\gamma} \alpha \vec{p}) + \vec{m} \times (\vec{m} \times (\alpha \vec{H}_{eff} - \frac{jg}{\gamma} \vec{p}))] \quad (1)$$

$$g = \frac{\hbar}{M_s * e * 2 * d} * \frac{P_r * \Lambda^2}{(\Lambda^2 + 1) + (\Lambda^2 - 1) * \cos(\angle(\vec{m}, \vec{p}))} \quad (2)$$

The parameters of equation (1), implemented in the software, were as follow: the gyromagnetic ratio  $\gamma$ , the Gilbert damping constant  $\alpha=0.01$ , the magnetocrystalline anizothropy constants  $K1=4.8 \cdot 10^4$  J/m<sup>3</sup>,  $K2=5.0 \cdot 10^3$  J/m<sup>3</sup> for Iron, the exchange constant  $A=2 \cdot 10^{-11}$  J/m, and the saturation magnetization  $M_s=2.1$  T [13, 14]. Constants used for scaling function (Eq. 2) calculations were as follows:  $e$  is the elementary electron charge,  $\hbar$  is the Planck constant. The  $d/P_r=3.33$  factor was calculated using the probe thickness  $d$ , and the polarization spin constant  $P$ . The  $\Lambda$  parameter was set to 1.6 [12]. The simulations were performed in such way that 16 different magnetization distribution were found for local energetic minima during the processes of minimization. Next, polynomial interpolation [15] was applied using the 3-rd degree polynomials, where for their determination, the time first degree derivative vanishing conditions were used in quasi-stable magnetization distribution points – interpolation of nodes for all finite element vertexes. Based on the interpolation polynomials the transition magnetization distribution as a function of time was obtained, while the first degree time derivatives were vanishing in the interpolated nodes. Thanks to this the vanishing conditions for the Slonczewski term were fulfilled in quasi-stable points of magnetization distributions reaching the adequate energy minima. Based on transient time distributions, for each moment  $t$  of the transient state, for which the integration algorithm determined the simulation step, the Slonczewski term values were calculated, for an each finite element vertex. In the same step, using Eq. 2, the values (different for each finite element vertex) of current density and polarization direction expressed in spherical coordinates (angles: theta, phi) were obtained. These values (averaged - the same for an each finite element vertex) were used for calculation using Eq.2) of new Slonczewski term. New Slonczewski term then was applied as the system excitation signal. After application of the Slonczewski term, it was checked if there existed a transition from the quasi-stable magnetization distribution, in

first energetic minimum, to the magnetization distribution in the targeted energetic minimum and what was the total energy deviation from the targeted energy level. The duration time of transitions was set up between 1 ps and 5 ps.

### III. RESULTS AND DISCUSSION

In Fig. 2(g-h) the maps are shown that present the geometrical parameters domain (green colour) for which the 16 quasi – stable energetic states (4 bits memory cell) exist, what means the total energy reaches the local minimum. For the considered types of cell the key role plays in an adjustment of the cutting angle – the alpha shown in Fig. 2f. As one can see, this parameter determines the area of 16 quasi-stable cases, for equivalent sections changing from 0 to 52.2 angular degree. This area depends on the probe radius or vertexes number in a little way. But the probe surface vertexes number, the probe radius, and slightly the alpha angle, have influence on maximal value of current density which changes the system state and the maximal total energy deviation what is presented in Fig. 3 and Fig. 5. The key parameter in this case is the time-duration of transitions among quasi-stable states which increases the maximal current densities values with its decrease. The current density which changes the system state, which is maximal from all maximums on the maps, exists for 36 surface vertexes probe, for the transition time 1 ps (Fig. 3 b) and it reaches the value of  $1.2 \cdot 10^{15}$  A/m<sup>2</sup>. The minimal current density, among all maximal current densities, exists for 100 surface vertexes probe, for time equals 5 ps (Fig. 3 c) and it doesn't exceed the value of  $3.9 \cdot 10^{14}$  A/m<sup>2</sup>. What concerns the total energy deviations, they are maximal for 36 surface-vertexes probe, for the time equals 1 ps (Fig. 5 b) and they don't exceed the 0.6% level. The least deviations

were received for 100 surface-vertexes probe (Fig. 5 c) don't exceed the 0.2% level. On Fig. 3 c the “e” point of maximal value from Fig. 4 b for 100 surface vertexes-probe with radius – 0.95 nm and alpha angle – 0 degree, is shown. This is maximal current density value from all transition combinations among 16 quasi-stable states for considered probe. On the map from Fig. 4a, it was shown that this value is the biggest from all 240 map values (the brightest colour) and it determines the transition from the state number 12 to the stable state number 16. Similar indication was applied in Fig. 5c where point “e” was highlighted. It is the point for the probe with geometrical parameters like above but it determines the percentage maximal total energy deviation which is obtained during simulation from targeted total energy in local energetic minimum. This deviation is maximal from all 240 cases of transitions for considered probe and it comes for transition from stable state 1 to stable state number 2. Making comparison between 36 surface vertexes probes and 100 surface vertexes probes one should focus on fact that 100 surface vertexes probes are better for future experimental or industrial applications according to lesser maximal current densities requirements in a case of the system state changing, for shorter transition times, and above all, according to lesser level of maximal total energy deviations. This behaviour is probably linked to the fact that considered probes have better geometrical symmetry in comparison to 36 surface vertexes probes. That's why the application of space homogeneous (the same values for all finite element vertexes) current densities and electron spin polarization for system excitation leads to lesser percentage energy deviation. Additionally according to probe radius decrease one receives the lesser maximal current densities values located in maximums of current densities curves.

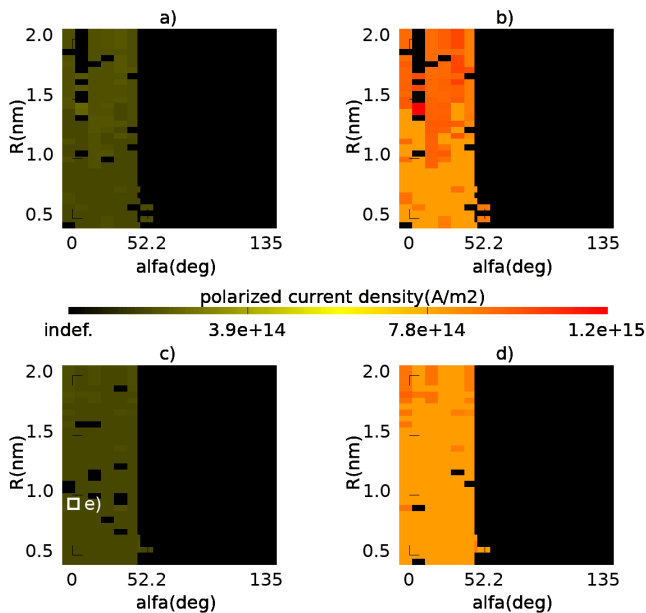


Fig. 3. The maximal values maps of current density maximums for all 240 quasi-stable states transitions for considered geometrical parameters: cells with 36 vertexes for transition times 5 ps (a) and 1 ps respectively (b), cell with 100 vertexes for transition times 5 ps (c) and 1 ps respectively (d). Point “e” on the map is the value in maximum on Fig. 4b and the brightest color on the map on Fig. 4a (switching from the state 12 to state 16) for the cell with 100 vertexes, radius 0.95 nm and the angle alpha of 0 angular degree.

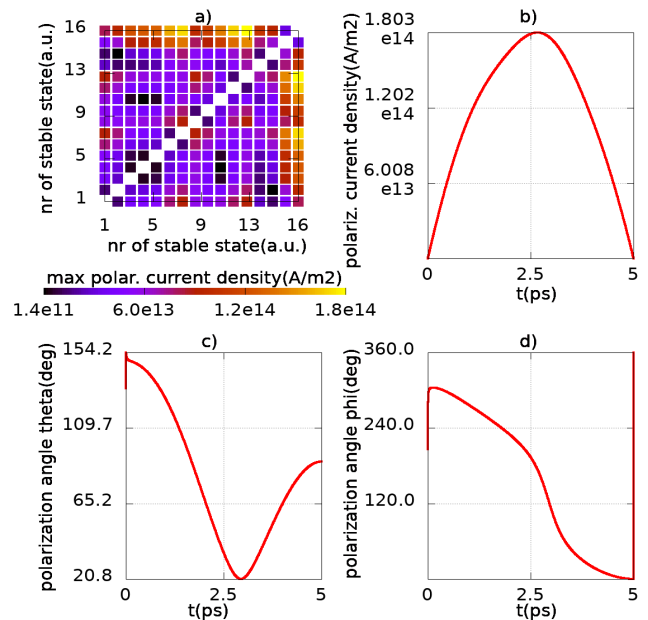


Fig. 4. Maximal current density values map for all (240) quasi – stable states transitions combinations for cell which has 100 vertexes, radius 0.95 nm and cutting angle alpha 0.0 degree (a). For this cell and for the switching from state 12 to state 16 - the current density time graph (b). The spherical coordinates of current polarization: theta (c), phi (d), respectively. For this transition, the current density has the highest value in maximum taken from all considered 240 transitions and this value is marked on Fig. 3c by the “e”, and it has the brightest color on the above map (a).

## IV. SUMMARY

The magnetic probes models group was examined. The group had different geometrical properties and it was examined for two different times duration for transitions among quasi – stable magnetization distributions which are found in system energy minimums. The geometrical parameters (radii and cutting angles – the shape angles) range was found. For this range, for each sample the 16 quasi-stable energetic states exist. This fact can be used for the 4 bits magnetic cells systems creation. The system excitations signals like time dependant current densities and the electron spin polarization directions were found for all cases of transitions among quasi–stable states. For the examined 16-state-cells, with the least geometrical area, the 300 times bigger writing density was achieved in comparison to the up to the date solutions. In matrices of such cells the real writing densities will be a little lesser because of dipolar interactions among cells what can be suppressed by increased distance between the cells. The time durations of transitions among quasi–stable states, which were used during simulations, increases the speed of memory input – output operations significantly (about 100 000 times faster) in comparison to actual semiconductor solutions.

It should be mentioned that the proposed memory model has to determine the aim which the electronic devices creation technology should evolve toward in nearest future. According to this fact, the very important factor, that can significantly impact on the model performance, is the samples preparation precision which focuses on the surface preparation and the acceptable deviations of it.

## REFERENCES

- [1] J. Akerman, „Toward a Universal Memory”, *Science* 308, 2005, pp. 508-510.
- [2] S. S. P. Parkin, M. Hayashi, L. Thomas, „Magnetic Domain-Wall Racetrack Memory”, *Science* 320, 2008, pp. 190-194.
- [3] T. Kawahara, K. Ito, R. Takemura, H. Ohno, „Spin-transfer torque RAM technology: Review and prospect”, *Microelectronics Reliability* 52, 2012, pp. 613-627.
- [4] H. Richter, A. Dobin, O. Heinonen, K. Gao, R. Veerdonk, R. Lynch, J. Xue, D. Weller, P. Asselin, M. Erden, R. Brockie, „Recording on Bit-Patterned Media at Densities of 1 Tb/in<sup>2</sup> and Beyond” *IEEE Trans. Magn.* 42, 2006, pp. 2255-2260.
- [5] D.K. Koltsov, A.O. Adeqeqe, M.E. Welland, D. M. Tricker, „Single-Domain Circular Nanomagnets”, *Phys. Rev. Lett.* 83, 1999, 1042.
- [6] W. Zhang and S. Haas, „Phase diagram of magnetization reversal processes in nanorings” *Phys. Rev. B* 81, 2010, 064433.
- [7] K. He, D. J. Smith, and M. R. McCartney, „Effects of vertex chirality and shape anisotropy on magnetization reversal of Co nanorings (invited)”, *J. Appl. Phys.* 107, 2010, 09D307.
- [8] T. Blachowicz, A. Ehrmann, „Square nano-magnets as bit-patterned media with doubled possible data density” *Materials Today: Proceedings* 4 (2017) S226–S231.
- [9] T. Blachowicz, A. Ehrmann, P. Steblinski, L. Pawela, „Magnetization reversal in magnetic half-balls influenced by shape perturbations”, *J. Appl. Phys.* 108, 2010, 123906
- [10] W. Scholz, J. Fidler, T. Schrefl, D. Suess, R. Dittrich, H. Forster, V. Tsiantos, „Scalable parallel micromagnetic solvers for magnetic nanostructures” *Comput. Mater. Sci.* 28, 2003, 366.
- [11] A. Vansteenkiste, J. Leliaert, M. Dvornik, M. Helsen, F. Garcia-Sanchez, B. Van Waeyenberge, „The design and verification of MuMax3”, *AIP Advances* 4, 2014, 107133
- [12] R. Lehdorff, D. E. Bürgler, A. Kakay, R. Hertel, C. M. Schneider, „Spin-Transfer Induced Dynamic Modes in Single-Crystalline Fe–Ag–Fe Nanopillars”, *IEEE Trans. Magn.* 44, 2008, 1951.
- [13] E. F. Kneller and R. Hawig, „The exchange-spring magnet: a new material principle for permanent magnets”, *IEEE Trans. Magn.* 27, 1991, 3588.
- [14] S. Tehrani, B. Engel, J. M. Slaughter, E. Chen, M. DeHerrera, M. Durlam, P. Naji, R. Whig, J. Janesky, J. Calder, „Recent developments in magnetic tunnel junction MRAM”, *IEEE Trans. Magn.* 36, 2000, 2752.
- [15] Z. Fortuna, B. Macukow, J. Wąsowski, „Metody Numeryczne”, WNT, 1998, wydanie czwarte.

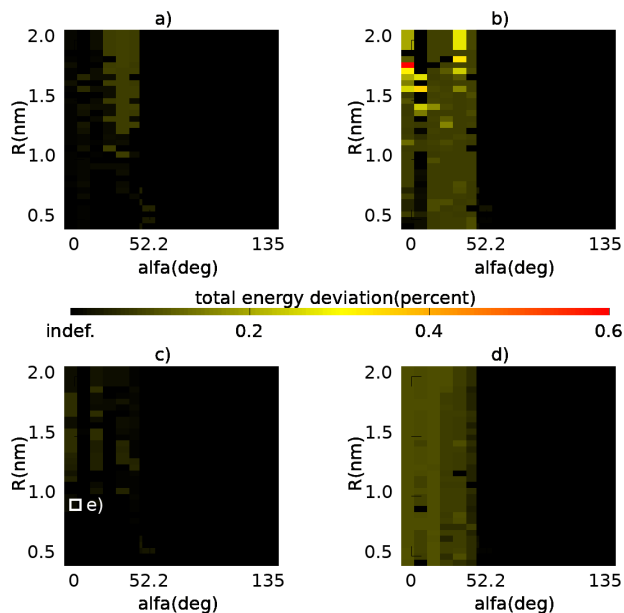


Fig. 5. Maximal total energy deviations maps for total energies in energetic minimums v.s. total energy after simulation: the object with 36 vertexes for transition times 5 ps (a) and 1 ps, respectively (b), the object with 100 vertexes for transition times 5 ps (c) and 1 ps (d), respectively. Point “e” on the map (c) marks the maximal deviation from all considered 240 transition combinations for the cell which has 100 vertexes, the radius 0.95 nm, and the cutting angle of 0 angular degree. This value is for transition from state 1 to state 2 and it doesn’t exceed 0.2 % value.